# Countering a fundamental law of attraction with quantum wave-packet engineering

G. Amit
*Faculty of Engineering and the Institute of Nanotechnology and Advanced Materials, Bar Ilan University, Ramat Gan 5290002, Israel and Soreq Nuclear Research Center, Yavne 81800, Israel*

Y. Japha, T. Shushi, and R. Folman
*Department of Physics, Ben-Gurion University of the Negev, Be'er Sheva 84105, Israel*

E. Cohen
*Faculty of Engineering and the Institute of Nanotechnology and Advanced Materials, Bar Ilan University, Ramat Gan 5290002, Israel*

(Received 22 October 2021; revised 4 December 2022; accepted 9 January 2023; published 27 February 2023)

Cold atoms hold much promise for the realization of quantum technologies, but still encounter many challenges. In this work we show how the fundamental Casimir-Polder force, by which atoms are attracted to a surface, may be temporarily suppressed by utilizing a specially designed quantum potential, which is familiar from the hydrodynamic or Bohmian reformulations of quantum mechanics. We show that when harnessing the quantum potential via suitable atomic wave-packet engineering, the absorption by the surface can be dramatically reduced. As a result, the probing time of the atoms as sensors can increase. This is proven both analytically and numerically. Furthermore, an experimental scheme is proposed for achieving the required shape for the atomic wave packet. All these may assist existing applications of cold atoms in metrology and sensing and may also enable prospective ones. Finally, these results shed light on the notion of quantum potential and its significance.

DOI: 10.1103/PhysRevResearch.5.013150

## I. INTRODUCTION

Quantum mechanics (QM) challenges our common sense. For example, it allows superposition states which we never see directly, it adheres to a minimal uncertainty principle, and it is nonlocal. This has brought its own founding fathers, such as Schrödinger, Einstein, and de Broglie, to speak against it. This has also given rise to many attempts to reinterpret it or even extend it. One of the attempts to reinterpret QM, and perhaps provide a base for future extensions of the theory, has been initially developed by de Broglie and Bohm and has been termed Bohmian mechanics (BM) [1–4]. Interestingly, several works have pointed out that employing BM could help solve complex numerical problems in QM [5–7]. However, the conceptual meaning and practical utility of this intriguing interpretation have apparently remained under debate.

In this paper we show that the Bohmian quantum potential (defined in the next section) enables the engineering of helpful scenarios. Specifically, we show how a fundamental force, the Casimir-Polder (CP) force, can be suppressed using this unique potential. This may enable new insights into the foundations of quantum theory, and may allow for new pathways in quantum technology applications, such as metrology and sensing. In particular, during the last two decades we have witnessed a major growth of experiments with cold atoms near surfaces. These experiments were driven by the desire to increase integration and scalability while miniaturizing these promising quantum devices, e.g., for various applications in metrology and atom interferometry [8,9]. The CP potential becomes important close to the surface, posing both fundamental and practical challenges. Recent works have utilized cold atoms to study the CP potential and examine atom-surface interactions [10–14].

We utilize the quantum potential $Q$, which depends only on the shape of the wave function, to propose a special engineering of atomic wave packets which enables them to partially resist the CP attraction.

Within the next two sections we analyze, first analytically and then numerically, the proposed wave-packet engineering and its performance. We then outline an experimental protocol for realizing this particular wave packet.

## II. SUPPRESSING THE CP FORCE VIA ATOMIC WAVE-PACKET SHAPING

In what follows, we propose a theoretical method to effectively suppress the CP force (for a limited amount of time) through the generation of a tailored quantum potential. This method can be simply described when applying the Madelung transformation [15] following the recent analyses in Refs. [16,17]. BM, as well as the Madelung formalism, allow to efficiently describe the interplay between external potentials and the quantum potential and hence we find them

very suitable in this case, where we try to counteract the former potentials.

We shall represent the wave function $\psi(\mathbf{r})$ in the polar form

$$\Psi(\mathbf{r},t) = \sqrt{\rho}(\mathbf{r},t)e^{iS(\mathbf{r},t)/\hbar}, \tag{1}$$

where $\rho$ and $S$ are the density and phase, respectively, and use the well-known guiding equation for the velocity

$$\mathbf{u} = \nabla\tilde{S}, \tag{2}$$

where the tilde superscript represents quantities per unit mass $m$, so that $\tilde{S} = \frac{S}{m}$. The real part of the Schrödinger equation then becomes the continuity equation

$$\frac{D}{Dt}\ln\rho = -\nabla\cdot\mathbf{u}, \tag{3}$$

where $\frac{D}{Dt} \equiv \frac{\partial}{\partial t} + \mathbf{u}\cdot\nabla$ is the material (Lagrangian) time derivative of a fluid element along its trajectory, and the imaginary part becomes

$$\frac{\partial\tilde{S}}{\partial t} = -(\tilde{K} + \tilde{Q} + \tilde{U}), \tag{4}$$

where $\tilde{K} = \mathbf{u}^2/2$ is the kinetic energy per unit mass and

$$\tilde{Q} = -\frac{\hbar^2}{2m^2}\frac{\nabla^2\sqrt{\rho}}{\sqrt{\rho}} \tag{5}$$

is the quantum potential per unit mass.

For an irrotational potential flow in the form of Eq. (2), we then obtain

$$\frac{D}{Dt}\mathbf{u} = -\nabla\tilde{Q}(\rho) - \nabla\tilde{U}, \tag{6}$$

suggesting the possibility of canceling an external potential $\tilde{U}$ using a suitable quantum potential $\tilde{Q}$.

Our proposed experimental setup consists of an atomic wave packet $\psi(x,z,t)$. At time $t = t_0$ the wave packet is brought close to the vicinity of a planar dielectric surface situated at $z = 0$ using a harmonic trap (see Fig. 1). For having a fair comparison between the Gaussian and engineered wave packets, we assumed that the harmonic trap remained active also for $t > 0$ in both, but in practice this has barely changed the simulation outcomes due to the much stronger CP potential.

A CP potential $U(\mathbf{r}) = -C_4/z^4$ acts on the atoms close to the dielectric surface, where $C_4$ is a constant depending on the properties of the surface and the atoms. Hereinafter we assume that the surface is the $z = 0$ plane. We further assume that the wave packet stays around the submicrometer distance from the surface but almost vanishes for very small distances from the surface, i.e., smaller than 100 nm from the surface, where the atom-surface interaction is dominated by the van der Waals potential, which has a $z^{-3}$ dependence. We focus below on the $z^{-4}$ potential which leads to a simple analytic solution for the engineered wave packet, but it turns out that the same wave packet can also resist the more realistic potential $U_1(\mathbf{r}) = -C_4/[z^3(z + 3\lambda_a/2\pi^2)]$ (also described in Ref. [20]), where $\lambda_a$ is the effective atomic transition wavelength (see the Appendix). We can therefore arrange the desirable situation $\frac{D}{Dt}\mathbf{u} = 0$, where the total acceleration of the atoms is zero, by preparing a density $\rho(\mathbf{r}) \equiv P^2(\mathbf{r})$, which

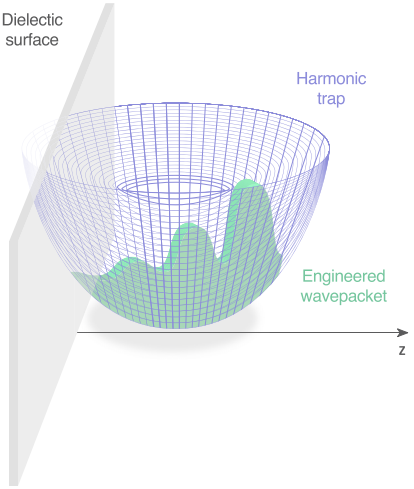


FIG. 1. Schematic illustration of the setup. A wave packet trapped in a harmonic potential is brought (together with the trap) close to a dielectric surface. The specific $z$ dependence of the wave packet is given by Eq. ( 9) and is depicted in Fig. 2

satisfies

$$\nabla^2 P + \frac{2mC_4}{\hbar^2 z^4}P = 0. \tag{7}$$

In our proposed experimental setup we are only interested in the dynamics along the $z$ axis and hence our problem becomes one-dimensional (1D). In 1D, the solution of the ordinary differential equation corresponding to Eq. (7) is

$$P(z) = z\left[C_1\cos\left(\frac{\sqrt{2mC_4}}{z\hbar}\right) + C_2\sin\left(\frac{\sqrt{2mC_4}}{z\hbar}\right)\right]. \tag{8}$$

See the Appendix for additional details. We note that this wave function is continuous at $z = 0$, i.e., on the surface, and vanishes there. This function is not always positive but the physically meaningful field $\rho$ is. Our numerical simulations below indicate a slightly inferior performance of $|P(z)|$ compared to $P(z)$ and thus we use it hereinafter.

We now have to properly truncate the wave function for making it realistic (and square-integrable). This can be done, for instance, by multiplying it with a Gaussian envelope, thus reaching a wave packet of the form

$$\psi(z) = ze^{-\frac{(z-z_0)^2}{4\sigma^2}}\left[C_1\cos\left(\frac{\sqrt{2mC_4}}{z\hbar}\right) + C_2\sin\left(\frac{\sqrt{2mC_4}}{z\hbar}\right)\right], \tag{9}$$

where the constants $z_0$ and $\sigma$ are the Gaussian's mean and width, respectively. A wave function having this density will spread with time, but as was shown in Ref. [17], $\tilde{Q}(\mathbf{r}, t + \Delta t) = \tilde{Q}(\mathbf{r}, t) + O[(\Delta t)^2]$. Therefore, an initial preparation of a wave function according to Eq. (9) is a good estimation for short times, which is the regime we will numerically simulate below. For longer times, the wave packet further spreads and becomes more and more distorted, thereby creating a different quantum potential which might be less beneficial. Using this technique a suitably prepared atomic wave packet

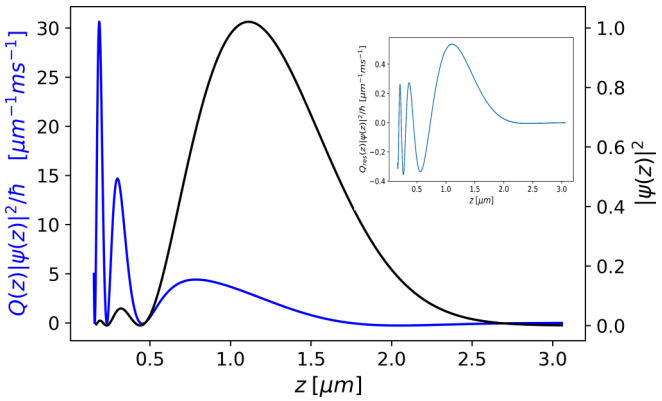


FIG. 2. The engineered wave packet and its quantum potential. The black curve describes the density of the engineered wave packet. The blue curve stands for the weighted quantum potential, namely, the quantum potential multiplied by the density of the engineered wave packet (divided here by $\hbar$). The inset presents the weighted residual potential, namely, the quantum potential together with the Casimir-Polder potential (ideally, these would have canceled each other completely, but the Gaussian envelope slightly changes that in a way captured by the residual potential), multiplied by the density of the engineered wave packet (same units). The negligible residue (about two orders of magnitude smaller than the Casimir-Polder potential) shows that indeed the quantum potential is able to successfully counter the Casimir-Polder potential, even with Gaussian truncation.

can be used, e.g., for measuring magnetic fields near the surface while passing above it, without being strongly drawn towards it.

For the short time spent by the wave packet in the vicinity of the surface, this kind of truncation was shown in a similar context to be almost innocuous [18]. In our case, it hinders the cancellation of the CP potential as calculated in the Appendix, but not fatally. The Gaussian truncation results in an unwanted *residual potential* (hereinafter there is no division by $m$ and hence no tildes are used) which is equal to

$$Q_{\rm res} = -\frac{\hbar^2}{2m\sigma^2}\left\{1 + \frac{z-z_0}{\sigma}\left[2\sigma\frac{P'(z)}{P(z)} - \frac{z-z_0}{\sigma}\right]\right\} \qquad (10)$$

Although the residual potential is not negligible, its largest component near $z = 0$ scales like $1/z^2$, hence it suggests a major improvement in comparison to the CP potential which scales like $1/z^4$ close to the surface. Figure 2 shows the weighted quantum potential, the weighted residual potential, and the density of the engineered wave packet.

Moreover, the inverse proportionality to $2\sigma^2$ guarantees that by increasing the width of the Gaussian envelope we can further shrink the overall size of the residual quantum potential. The term $P'(z)/P(z)$ is also diverging, but if we average over the region of each singularity we will get a small contribution (sometimes in the form of a favorable repulsive potential). Therefore, and in contrast to the unengineered Gaussian, where the atoms are strongly attracted to the surface, here they will not be attracted so strongly. On the other hand, they may suffer from irregularities in the vicinity of the singularities, and this is the reason that the numerical simulation performed below is important. Nevertheless, we may conclude on analytic grounds that while a solution of the form Eq. (8) could completely cancel the CP potential, the more realistic truncated shape in Eq. (9) also has the ability to suppress the CP force (for a limited amount of time).

Although we employed here the Madelung-Bohm formalism, as in Refs. [16,17], for finding a beneficial shape of the wave packet enabling hydrostatic equilibrium [19], Eq. (7) can be simply recognized as the Schrödinger equation once we require a stationary solution. Similarly, it seems to us helpful to analyze the residual potential in the current Madelung-Bohm formalism, but exactly the same considerations can be straightforwardly applied to the standard Schrödinger equation when inserting there the truncated wave packet. The two approaches trivially agree with each other, and indeed, within the next section we will present a numerical analysis employing the Schrödinger formalism.

## III. NUMERICAL SIMULATION

In order to study the performance of the proposed wave-packet engineering, we perform a numerical simulation examining the dynamics of the wave packet in the vicinity of a dielectric surface. In particular, we wish to examine how the absorption of particles evolves in time when using engineered and unengineered wave packets. The aim, of course, is to minimize the absorption when using an engineered wave packet. Essentially, we solve the time-dependent Schrödinger equation using the standard numerical solver in MATLAB.

To embed the proposed scheme within a more realistic setup, we are assuming that the atoms lie in a harmonic trap, situated close to the surface (throughout this work, the frequency of the harmonic trap is standardly determined by $\sigma$ and $m$). The atoms are initially at rest. In addition, to simulate the absorption in the surface we assume, similarly to Ref. [20], an imaginary (absorbing) potential $V_{\rm abs}$ growing linearly from zero at $z = \delta = 0.15\,\mu$m to $z = 0$, i.e., $V_{\rm abs} = iV_0(\delta - z)$ for $0 < z < \delta$ and otherwise 0, where $V_0 = 10^{-25}\,Jm^{-1}$. This implies that any atom that enters the region below $\delta = 0.15\,\mu$m is absorbed within a certain time, unless having a sufficiently large velocity in the other direction, while the real part of the potential remains constant throughout $0 < z < 0.15\,\mu$m (we do require continuity in $z = 0.15\,\mu$m). In most of the cases we examined, the atomic wave packet was prepared farther from the region $z < \delta$ and hence only a small fraction of its tail resided in the absorbing region.

This necessary modification of the total potential deteriorates the performance of our engineered wave packet, which was not originally meant to resist it. However, as we shall show below, the simulative rate of absorption exhibited by the engineered wave packet was still lower than that of the customary Gaussian wave packet, which is consistent with the fact that the residual potential is much smaller than the CP potential near the surface.

We consider a $^{87}$Rb atom (mass $m = 1.44 \times 10^{-25}$ kg) near a silicon surface (refractive index $n = 2$). For the ground state static polarizability of $^{87}$Rb [$\alpha_0 = 0.0794\,{\rm Hz/(V/cm)^2}$] we have $C_4 = 9.1 \times 10^{-56}$ J m$^4$. We now solve the time-dependent Schrödinger equation for the atoms under the influence of the CP + harmonic + absorbing potentials. Unlike the scattering scenario analyzed in Refs. [21,22], the

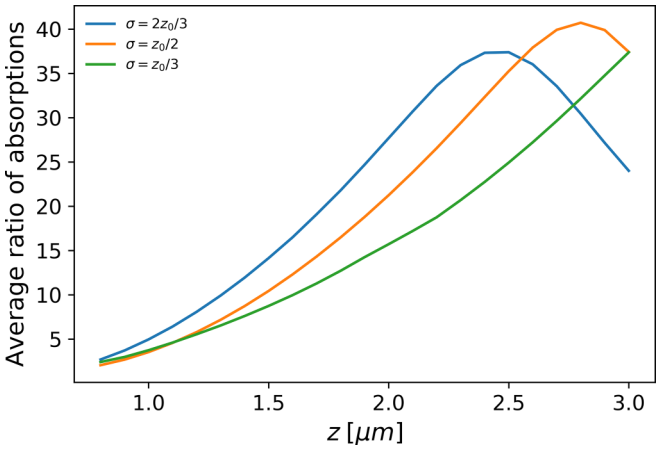


FIG. 3. Comparison, in terms of absorption, between the engineered wave packet and a Gaussian for various preparations of the wave packets. The average ratio (over the time interval $0 \leqslant t \leqslant 2$ ms) of the absorbed fractions is calculated (i.e., Gaussian wave-packet absorption divided by engineered wave-packet absorption) as a function of $z_0$, the mean position of the Gaussian envelope, while the ratio between the standard deviation and $z_0$ is kept constant (equal to either $2/3$, $1/2$, or $1/3$). As expected, at short times large standard deviation is preferable, but in all cases a substantial advantage is achieved.

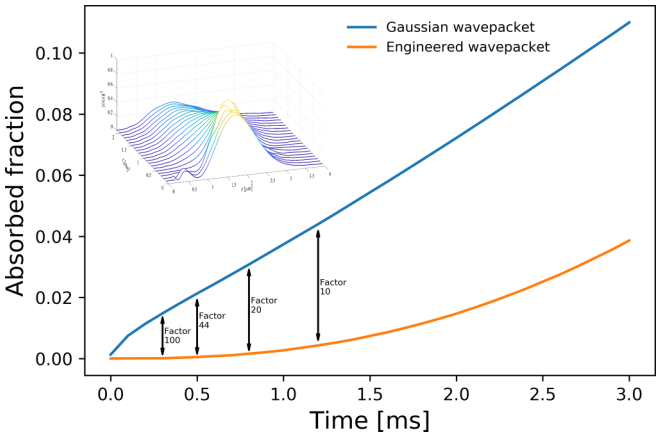


FIG. 4. Comparison between the engineered wave packet and a Gaussian over time for a specific choice of parameters. The mean and standard deviation of the Gaussian are chosen to be $z_0 = 3\ \mu$m and $\sigma = 1\ \mu$m, respectively, enabling a particularly beneficial performance (two orders of magnitude advantage at short times and one order of magnitude at longer times). The absorption rates of the two wave packets become comparable around 3 ms. The inset shows the time evolution of the engineered wave packet within the harmonic and Casimir-Polder potentials. As may be seen, the wave packet eventually loses its specially engineered shape, thus diminishing the effect countering the Casimir-Polder force. For this specific calculation, the parameters used for the mean and standard deviation of the Gaussian envelope were particularly challenging, $z_0 = 1\ \mu$m $\sigma = 2/3\ \mu$m, in order to emphasize the transient nature of the effect due to the external potentials.

atoms start from rest in our simulation and the dominant term is the negative potential energy dictating a bound state (as an example, the initial energy was $-1.95 \times 10^{-29}\,J$ for a typical wave packet of width $0.67\ \mu$m starting at $z = 1\ \mu$m from the surface). For this reason, absorption should be determined by the wave packet shape rather than quantum reflection. We run a simulation for a large set of means ($z_0$) and standard deviations ($\sigma$), and calculate the absorption fraction. Before the truncation, the sine and cosine solutions in Eq. (8) should give rise to the same quantum potential. However, the residual potential stemming from the truncation reveals that there is a difference between the two cases, and we indeed notice some advantage of the cosine solution over the sine.

We compare for various cases our proposed solution in Eq. (9) to a Gaussian wave packet with the same mean and standard deviation as those of the envelope (see Fig. 3). It is desirable to decrease as much as possible the residual potential, and since it contains three terms depending on $\sigma^{-2}$, $\sigma^{-3}$, and $\sigma^{-4}$, we have better results for higher-$\sigma$ wave packets. To further explore the advantage we choose some specific parameters ($z_0 = 2.3\ \mu$m and $\sigma = 1\ \mu$m) and compare the absorbed fractions (see Fig. 4). For a similar figure concerned with the potential $U_1$ please see the Appendix—the results again show a clear advantage.

As can be seen from Figs. 3 and 4, the engineered wave packet leads to a significantly smaller absorbed fraction, which implies that the CP force has less impact on our engineered wave packet in comparison to its impact on a Gaussian wave packet. Thus, the results show that the engineered wave packet's shape indeed has the ability to reduce the unwanted effects of the CP force. In accordance with our analytic expectations, the engineered wave packet excels at high standard deviations and short times, reaching in some cases a 100-fold advantage over the Gaussian wave packets in terms of absorption.

Note, however, that the engineered wave packet is typically skewed away from the surface in comparison to the Gaussian envelope (and hence in comparison to the Gaussian wave packet we used as a benchmark). Thus, one may ask whether the presented advantage follows only from this spatial displacement rather than the special shape of our wave packet. To test this hypothesis we tried to fit a Gaussian wave packet to the engineered solution by locating it farther away from the surface and/or shrinking its width until it highly resembled the Gaussian we compared it to. In all these cases we still found an advantage in favor of the engineered wave packet (albeit smaller). We present such a comparison in the Appendix, where we significantly pushed the Gaussian away from the surface. We still found that the engineered wave packet has a substantially smaller absorbed fraction. Thus, we conclude that not only the shifted mean and modified width but also the particular shape of the wave packet contributed to the observed advantage.

Finally, we discuss the transient nature of the effect. As can be seen in Fig. 4, the absorption rate of the engineered wave packet shows no advantage after about 3 ms. This is due to the fact that with time it loses its unique shape which originally gave rise to the required quantum potential. To show this explicitly, we plot in the inset of Fig. 4 the time evolution of the engineered solution from Eq. (9) with $z_0 = 1\ \mu$m and $\sigma = 2/3\ \mu$m. We can clearly see the amplitude decreasing with time and the shape being distorted.

## IV. A POSSIBLE SCHEME FOR ACHIEVING THE REQUIRED WAVE-PACKET ENGINEERING

As was shown in the previous section, a certain shape of the wave packet provides the desirable result, i.e., resisting the CP force for a short time. The construction of such a wave packet can be obtained in several ways. We discuss here in general terms a technique which utilizes external potentials and fields (resembling Refs. [23] and [24]). In practice, this preparatory stage should precede the aforementioned evolution close to the surface and should be performed in a controlled environment.

First, a Gaussian atomic wave packet can be prepared by cooling the atoms to occupy the Gaussian ground state of a harmonic potential. Engineering the wave packet to the form of Eq. (9) may be done in two stages by utilizing an interferometric sequence with two internal atomic states having a different response to an external potential, e.g., due to a magnetic field. We use a magnetic field gradient pulse of duration $T$ to create a state-dependent spatially varying potential sandwiched between two properly designed Rabi pulses inducing transitions between the two states. These would be followed by a projection to one state, transforming the atomic wave packet as $\psi(z) \to \psi(z)[ae^{i\varphi(z)} + be^{-i\varphi(z)}]$. Here $\varphi(z) = \delta V(z)T/2\hbar$ is the phase imprinted by the short pulse of potential difference $\delta V(z)$ between the two atomic states, while $a$ and $b$ are complex numbers determined by the Rabi pulses (we neglect a possible space-dependent global phase). In order to generate the linear $z$ dependence in front of the right-hand side of Eq. (9) we can apply a linear potential difference $\delta V(z) = Fz$, choose $b = -a$, and obtain $\psi(z) \to \psi(z)\sin(Kz) \approx Kz\psi(z)$ (if $Kz = FTz/2\hbar \ll 1$). For generating any superposition of the cosine and sine dependence with an argument proportional to $1/z$ we can apply a differential potential with a $1/z$ dependence, e.g., a magnetic field generated by a current-carrying wire on the surface, and choose $|a| = |b|$ with a certain phase difference that determines the coefficients of the superposition of the cosine and sine functions.

The resulting wave packet, serving as a good approximation to Eq. (9) (for $z > 0$), could now be used, e.g., as an input for magnetometry applications near the dielectric surface without being strongly attracted to it. Magnetometry can be performed with $F = 1$ or $F = 2$ spin or Bose-Einstein condensate (BEC) atoms and is often shot-noise limited [25,26]. Increasing the number of nonabsorbed atoms using the proposed method could therefore be expected to improve the precision in a manner proportional to the square root of the above average ratio of absorptions. The challenge would be to sustain the engineered wave packet for a relatively long period of time, but judging by the advantageous trend in Fig. 4 this could be possible (bearing in mind that the distance from the surface is typically larger than in our simulation).

Our 1D model is suitable for describing an atom-surface potential that varies only in the direction perpendicular to the surface. However, for analyzing a realistic situation it will be necessary to take into account the 3D nature of the atomic wave packet, which is manipulated, for example, by magnetic fields that vary in 3D. In particular, a precise design of the chip-based system of wires or magnets used to manipulate the atoms will have to be carried out. In addition, the detection of the state of the atoms after the process near the surface may also be challenging and cannot be described within the scope of the current work.

## V. DISCUSSION

We explored the possibility to use the Bohmian potential in order to cancel external potentials via wave-packet shaping. We have analytically proposed a technique that allows to suppress the CP force (for a limited period of time) and tested it numerically. Using this approach, we examined the case in which a Gaussian wave packet is engineered into a special form such that near a dielectric surface the wave packet resists the CP force. We have addressed the case of a wave packet brought to a surface using a harmonic trap, but the presented analysis can be readily generalized to a grazing beam scenario (such as Ref. [14]). Although being related in the past to *surreal* phenomena, this work emphasizes the very *real* effects of the quantum potential, as well as its possible applications in practical scenarios. In addition to providing insight concerning the Bohmian interpretation, this analysis may pave the way for various applications, e.g., surface magnetometry with cold atoms having engineered wave packets which can survive longer at the vicinity of the surface. Although the CP potential was analyzed above, it should be noted that the useful interplay between external potentials and the quantum potential is general. Therefore, by carefully engineering the wave packet, it is possible to suppress additional forces such as the gravitational or van der Waals forces.

## ACKNOWLEDGMENTS

The authors wish to thank numerous colleagues for helpful discussions, and in particular, Eli Pollak, Daniel Rohrlich, Shim'on Sukholuski, and Yaara Shaked for their helpful comments and support. This work was funded in part by the Israel Science Foundation (Grants No. 856/18 and No. 1314/19), the DFG through the DIP program (Grant No. 703/2-1), the Israel Innovation Authority (Grants No. 70002 and No. 73795), Elta Systems Ltd., the Israeli Council for Higher Education, the Pazy Foundation, and the Israeli Ministry of Science and Technology. This research was supported by Grant No. FQXi-RFP-CPW-2006 from the Foundational Questions Institute and the Fetzer Franklin Fund, a donor-advised fund of the Silicon Valley Community Foundation.

## APPENDIX

### 1. The engineered wave packet and the total potential

The engineered wave packet we employed is given by the solution of

$$\nabla^2 P + \frac{2mC_4}{\hbar^2 z^4} P = 0, \tag{A1}$$

multiplied by a Gaussian truncation $e^{-\frac{(z-z_0)^2}{4\sigma^2}}$, yielding

$$\psi(z) = ze^{-\frac{(z-z_0)^2}{4\sigma^2}}\left[C_1\cos\left(\frac{\sqrt{2mC_4}}{z\hbar}\right) + C_2\sin\left(\frac{\sqrt{2mC_4}}{z\hbar}\right)\right]. \tag{A2}$$

In our numerical simulation we assumed that the wave packet is brought to the vicinity of the dielectric surface using

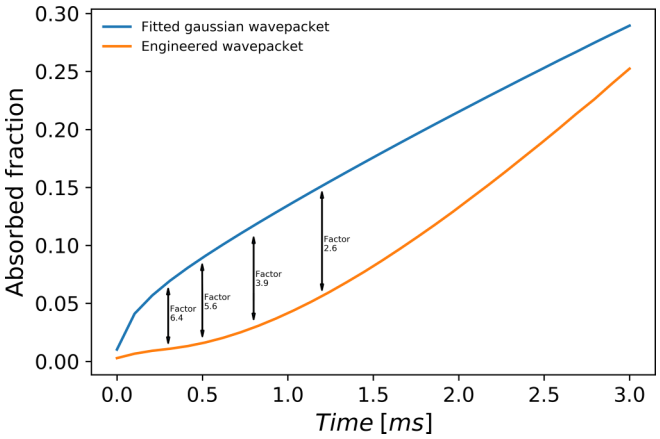


FIG. 5. Comparison between an engineered wave packet and a fitted Gaussian over time for a specific choice of parameters. The mean and standard deviation of the Gaussian are chosen to be $z_0 = 2.3\,\mu\text{m}$ and $\sigma = 1\,\mu\text{m}$, respectively, while the corresponding parameters of the engineered wave packet are $z_0 = 1.43\,\mu\text{m}$ and $\sigma = 1\,\mu\text{m}$. Despite the significantly improved parameters of the Gaussian, the engineered wave packet maintains a substantial advantage.

a harmonic potential which remains there. Then, following Ref. [20], the Casimir-Polder potential $V_{\text{CP}}(z)$ is acting on the wave packet for any $z \geqslant 0.15\,\mu\text{m}$. For $0 < z < 0.15\,\mu\text{m}$ it is replaced by a constant value, $V_{\text{CP}}(0.15)$ (assuring continuity at $z = 0.15\,\mu\text{m}$), and a linear imaginary potential is added as in Ref. [20].

### 2. Calculation of the residual potential

We shall compute here the residual quantum potential corresponding to our proposed construction. This will allow us to investigate more deeply the analytic properties of the shaping, which are important for any experimental demonstration of this technique.

In 1D, the solution of our ordinary differential equation takes the form (A2). For simplicity we define the following function:

$$\alpha(z) = \left[C_1 \cos\left(\frac{\sqrt{2mC_4}}{z\hbar}\right) + C_2 \sin\left(\frac{\sqrt{2mC_4}}{z\hbar}\right)\right]. \quad \text{(A3)}$$

We shall now compute the value of

$$\chi = \frac{d^2}{dz^2}\left[e^{-(z-z_0)^2/\zeta} z\alpha(z)\right] + \frac{2mC_4}{\hbar^2 z^4}\left[e^{-(z-z_0)^2/\zeta} z\alpha(z)\right], \quad \text{(A4)}$$

where $\zeta = 4\sigma^2$. That is,

$$\chi = \frac{d}{dz}\left(\frac{d}{dz} z e^{-(z-z_0)^2/\zeta}\alpha(z)\right) + \frac{2mC_4}{\hbar^2 z^4} z e^{-(z-z_0)^2/\zeta}\alpha(z), \quad \text{(A5)}$$

and after some algebraic calculations,

$$\chi = e^{-(z-z_0)^2/\zeta}\left[-\frac{2}{\zeta}3z\alpha(z) - 2z_0\alpha(z) + z^2\alpha'(z) - zz_0\alpha'(z) + z(z-z_0)\alpha'(z) + \frac{4}{\zeta^2}z(z-z_0)^2\alpha(z) + z\alpha''(z) + \frac{2mC_4}{\hbar^2 z^3}\alpha(z) + 2\alpha'(z)\right]. \quad \text{(A6)}$$

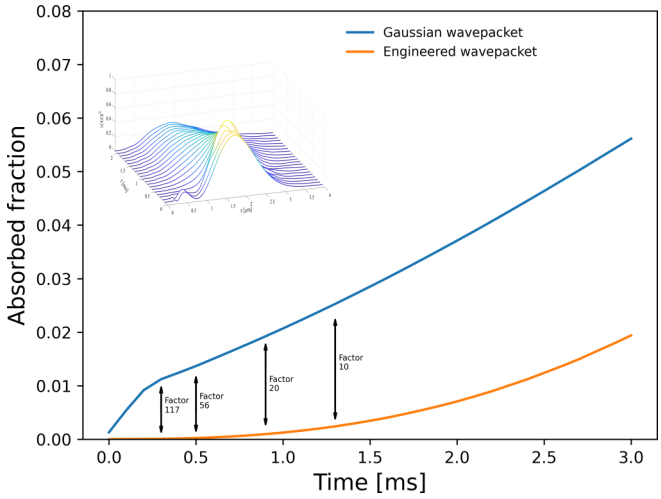


FIG. 6. Comparison between an engineered wave packet and a Gaussian in case of a more realistic potential. All parameters are identical to those used in Fig. 4 of the main text, but instead of a simple $z^{-4}$ potential, the $U_1$ potential described above was used.

From the fact that $\frac{2mC_4}{\hbar^2 z^3}\alpha(z) + 2\alpha'(z) + z\alpha''(z) = 0$, we have

$$\chi = \frac{e^{-(z-z_0)^2/\zeta}}{\zeta}[(-6z + 4z_0)\alpha(z) - 4z(z-z_0)\alpha'(z) + \frac{4}{\zeta}z(z-z_0)^2\alpha(z)]. \quad \text{(A7)}$$

This suggests that the residual quantum potential is

$$Q_{\text{res}} = \frac{\hbar^2}{2m}\left[\frac{-6 + 4z_0/z - 4(z-z_0)\alpha'(z)/\alpha(z)}{\zeta} + \frac{4(z-z_0)^2}{\zeta^2}\right].$$

This can be written more shortly as

$$Q_{\text{res}} = -\frac{\hbar^2}{2m\sigma^2}\left\{1 + \frac{z-z_0}{\sigma}\left[2\sigma\frac{P'(z)}{P(z)} - \frac{z-z_0}{\sigma}\right]\right\},$$

where $P(z) = z\alpha(z)$ is the original function defined in Eq. (8) of the main text. The above expression coincides with Eq. (10) there.

### 3. Comparison to a fitted Gaussian

To verify that the advantage reported above (in terms of absorption) stems from the shape and not only the bias of the engineered wave packet away from the surface, we compare in Fig. 5 the absorption of the engineered solution to the absorption of a fitted Gaussian located at the same distance from the dielectric surface. The advantage is smaller, but still apparent.

### 4. Countering a more realistic potential

We tested the proposed wave-packet engineering method also in the case of the following potential [20]: $U_1(\mathbf{r}) = -C_4/[z^3(z + 3\lambda_a/2\pi^2)]$. The results and (beneficial) comparison to a Gaussian wave packet are presented in Fig. 6.

[1] D. Bohm, A suggested interpretation of the quantum theory in terms of "hidden" variables. I, Phys. Rev. **85**, 166 (1952).

[2] D. Bohm and B. J. Hiley, *The Undivided Universe: An Ontological Interpretation of Quantum Theory* (Routledge, London, 1993).

[3] P. R. Holland, *The Quantum Theory of Motion: An Account of the de Broglie-Bohm Causal Interpretation of Quantum Mechanics* (Cambridge University Press, Cambridge, 1993).

[4] J. T. Cushing, A. Fine, and S. Goldstein, *Bohmian Mechanics and Quantum Theory: An Appraisal* (Springer Science and Business Media, Dordrecht, 1996).

[5] A. S. Sanz and S. Miret-Artés, Setting up tunneling conditions by means of Bohmian mechanics, J. Phys. A: Math. Theor. **44**, 485301 (2011).

[6] P. Botheron and B. Pons, Self-consistent Bohmian description of strong field-driven electron dynamics, Phys. Rev. A **82**, 021404(R) (2010).

[7] S. Garashchuk, J. Mazzuca, and T. Vazhappilly, Efficient quantum trajectory representation of wavefunctions evolving in imaginary time, J. Chem. Phys. **135**, 034104 (2011).

[8] J. Fortágh and C. Zimmermann, Magnetic microtraps for ultracold atoms, Rev. Mod. Phys. **79**, 235 (2007).

[9] M. Keil, O. Amit, S. Zhou, S. Groswasser, Y. Japha, and R. Folman, Fifteen years of cold matter on the atom chip: Promise, realizations, and prospects, J. Mod. Opt. **63**, 1840 (2016).

[10] Y. J. Lin, I. Teper, C. Chin, and V. Vuletić, Impact of the Casimir-Polder Potential and Johnson Noise on Bose-Einstein Condensate Stability Near Surfaces, Phys. Rev. Lett. **92**, 050404 (2004).

[11] T. A. Pasquini, M. Saba, G.-B. Jo, Y. Shin, W. Ketterle, D. E. Pritchard, T. A. Savas, and N. Mulders, Low Velocity Quantum Reflection of Bose-Einstein Condensates, Phys. Rev. Lett. **97**, 093201 (2006).

[12] J. M. Obrecht, R. J. Wild, M. Antezza, L. P. Pitaevskii, S. Stringari, and E. A. Cornell, Measurement of the Temperature Dependence of the Casimir-Polder Force, Phys. Rev. Lett. **98**, 063201 (2007).

[13] D. A. R. Dalvit, P. A. M. Neto, A. Lambrecht, and S. Reynaud, Probing Quantum-Vacuum Geometrical Effects with Cold Atoms, Phys. Rev. Lett. **100**, 040405 (2008).

[14] B. S. Zhao, H. C. Schewe, G. Meijer, and W. Schöllkopf, Coherent Reflection of He Atom Beams from Rough Surfaces at Grazing Incidence, Phys. Rev. Lett. **105**, 133203 (2010).

[15] E. Madelung, Quantentheorie in hydrodynamischer Form, Z. Phys. **40**, 322 (1927).

[16] E. Heifetz and E. Cohen, Toward a thermo-hydrodynamic like description of Schrödinger equation via the Madelung formulation and Fisher information, Found. Phys. **45**, 1514 (2015).

[17] M. de Gosson, B. Hiley, and E. Cohen, Observing quantum trajectories: From Mott's problem to quantum Zeno effect and back, Ann. Phys. **374**, 190 (2016).

[18] G. A. Siviloglou, J. Broky, A. Dogariu, and D. N. Christodoulides, Observation of Accelerating Airy Beams, Phys. Rev. Lett. **99**, 213901 (2007).

[19] E. Heifetz and I. Plochotnikov, Madelung transformation of the quantum bouncer problem, Europhys. Lett. **130**, 10002 (2020).

[20] R. G. Scott, A. M. Martin, T. M. Fromhold, and F. W. Sheard, Anomalous Quantum Reflection of Bose-Einstein Condensates from a Silicon Surface: The Role of Dynamical Excitations, Phys. Rev. Lett. **95**, 073201 (2005).

[21] S. Miret-Artes and E. Pollak, Scattering of He atoms from a microstructured grating: Quantum reflection probabilities and diffraction patterns, J. Phys. Chem. Lett. **8**, 1009 (2017).

[22] J. Petersen, E. Pollak, and S. Miret-Artes, Quantum threshold reflection is not a consequence of a region of the long-range attractive potential with rapidly varying de Broglie wavelength, Phys. Rev. A **97**, 042102 (2018).

[23] M. Nest, Y. Japha, R. Folman, and R. Kosloff, Dynamic matter-wave pulse shaping, Phys. Rev. A **81**, 043632 (2010).

[24] Y. Margalit, O. Dobkowski, Z. Zhou, O. Amit, Y. Japha, S. Moukouri, D. Rohrlich, A. Mazumdar, S. Bose, C. Henkel, and R. Folman, Realization of a complete Stern-Gerlach interferometer: Toward a test of quantum gravity, Sci. Adv. **7**, eabg2879 (2021).

[25] M. Vengalattore, J. M. Higbie, S. R. Leslie, J. Guzman, L. E. Sadler, and D. M. Stamper-Kurn, High-Resolution Magnetometry with a Spinor Bose-Einstein Condensate, Phys. Rev. Lett. **98**, 200801 (2007).

[26] Y. Eto, H. Ikeda, H. Suzuki, S. Hasegawa, Y. Tomiyama, S. Sekine, M. Sadgrove, and T. Hirano, Spin-echo-based magnetometry with spinor Bose-Einstein condensates, Phys. Rev. A **88**, 031602(R) (2013).